ISSN: 2476- 2334

Research Article

International Journal of Nanotechnology & Nanomedicine

Morphological and Raman Study of an Anodized Tio_2 Nanotubular Matrix without Presence of Nanograss, Using Graphite as Cathode

Marcos Luna Cervantes*, Adriana Báez Rodríguez, Julián Hernández Torres and Luis Zamora Peredo

Centro de Investigación en Micro y Nanotecnología, Universidad Veracruzana, Adolfo Ruiz Cortines 455, C.P. 94294, Boca del Río, México.

***Corresponding author**

Marcos Luna Cervantes, Centro de Investigación en Micro y Nanotecnología, Universidad Veracruzana, Adolfo Ruiz Cortines 455, C.P. 94294, Boca del Río, México.E-mail: marcos_luna_c@hotmail.com

Submitted: 14 June 2018; **Accepted**: 20 June 2018; **Published**: 27 June 2018

Abstract

One set of TiO_2 nanotubes is anodized to identify and study the time lapse of a matrix of them without presence of nanograss as a residual layer. The anodization process consists of an organic media of ethylene glycol and NH_4F salts, constant voltage for a time period from 10 to 60 minutes. All anodized samples are rinsed and annealed to 400 °C by 2 hours to obtain an anatase crystalline structure. The morphological characterization was carried out by Field Emission Scanning Electron Microscopy to verify the presence of the nanotubes and calculate the surface roughness factor and film porosity. It was observed that roughness factor and porosity doesn't have important variations, as time function, except for 60 minutes where nanograss has a strong presence and the gaps between nanotubes are minimal. Raman Spectroscopy was used for optical characterization in order to identify the changes in signal intensity and Eg mode Shift associated with anodization time. It was observed that intensity suffers an increment and Eg mode Shift suffers a decrement as thickness function (anodization time).

Keywords: TiO_2, nanotube, nanograss, anatase,anodization, graphite, Raman.

Introduction

Metal oxide nanostructures are of considerable interest due to their properties like a high volume-area ratio as a very important property of nanoscale and a new family of structures has been developed, named by what they look like, e. g. nanosheets, nanograss, nanoribs, nanorods, nanopores, nanowires, nanobelts and so on [1,2]. Within this family, there is one special type of nanostructure which has in fact a double surface area that offers one direct and efficient pathway for electron transport and more available area for nanoparticles insertion they are called nanotubes [3-5].

Nowadays, Titania nanotubes (TNTs) has a strong presence in many scientific and industrial study fields and applications like photo electrolysis, dye-sensitized solar cells, photocatalytic reduction of CO_2, biomedical applications: biosensors and, drug delivery, due to its properties such as non-toxic, environmentally friendly, optical and electronic properties [6-10].

TiO_2 nanotubes can be synthesized using anodic oxidation process, more generally called as anodization, first reported in 2001 for titanium dioxide [11]. This versatile technique uses titanium (anode) and, commonly, a plate, rod or foil of pure platinum as cathode, this material is too expensive. Anodization takes commonly hours [12,13].The anodized samples are cleaned frequently, using a mechanical method (e.g. ultrasonic bath), even when the nanotubes suffer some alteration in their shape or top layer surface, to remove the residual structures such nanograss, sponge or just a thin oxide layer, prolonged time or high concentration of salts can cause it happen [14,15]. As-anodized oxide layer formed, it is amorphous in nature, generally, crystallization is achieved through thermal treatment at 300-500 °C in a variety of atmospheres for high performance applications with anatase phase [16-18].

The roughness factor, that is, the physical surface area of the film per unit projected area, measures the internal surface area of the electrode and is of crucial significance in applications such as sensing and catalysis. It is essential to calculate the roughness factor (Rf) and porosity (P) to handle nanotubes application, such as dye absorbing for dye-sensitized solar cells and gas sensor, both are calculated from geometrical parameters [19].

The main goal of this study was to identify the time lapse, in minutes, where a TiO_2 nanotubular matrix is obtained with no presence of nanograss, and exclude the ultrasonic bath or another mechanical method to remove it. A good tube shape, a vertical alignment and a free top layer, are necessary characteristics for a better performance in almost all applications; moreover, an important factor in this study was the selection and use of graphite as an effective alternative cathode, due to low cost and optimal nanotube morphology.

Methods

Titanium foils (15x15x0.1mm) were firstly used as an anodic electrode, while pure graphite rods (35x6mm) were used as cathodic

electrode. Titanium foils were cut in smaller foils (15x5x0.1mm), then they were cleaned by ultra-sonication successively in ethanol, deionized water and acetone. The distance between electrodes was constant in every experiment (30mm). The foils were anodized from 10 to 60 minutes in organic electrolyte: ethylene glycol, 2% deionized water and 1.2 wt% NH_4F; using two electrode configurations. The anodization was carried out using a DC power source under constant voltage of 30 V.

After anodization process, the whole set of anodized samples was rinsed in deionized water, dried and then annealed at 400 °C for 4 hours in air. The morphology and structure of TiO_2 nanostructure was characterized by Field Emission Scanning Electron Microscope (JSM-7600F, JEOL), Raman spectra were obtained on a DXR Raman Microscope (Thermo Scientific) using a 532 nm laser.

Results and discussions

Inner diameter, outer diameter, center to center (tubes) are obtained from SEM images for geometrical considerations, as Figure 1 shows. Mainly, Figure 2, lets to see how nanotubes layer suffers a several change just in top surface. An increment exists in the inner and outer diameter due to time progress. Attending to shape and free top surface, There are in a), b) and c), a good nanotube layer with a little presence of residual thin oxide, result of the first stage of growth (10, 20 and 30 minutes of anodization respectively) [20]. d) Lets to see how the nanotubes starts to collapse forming clusters of bundled nanotubes (also called nanotube islands), which could be produced during the anodization process or during the cleaning and evaporative drying process of the as-deposited films through capillary forces of the liquid, acting between the nanotubes [21]. e) Nanograss starts to appear over top layer of tube; f) Now, nanograss has a strong presence and it can increase the Raman signal due to surface contact.

Figure 3, presents two near SEM perspective, a) for 10 minutes with 335 nanometers average tube length, b) 50 minutes with 679 nanometers average tube length, c) distant perspective for 30 minutes, here it is possible to see the highest covered area; to remark, the tube length suffers an increment when the anodizing time is increasing as well.

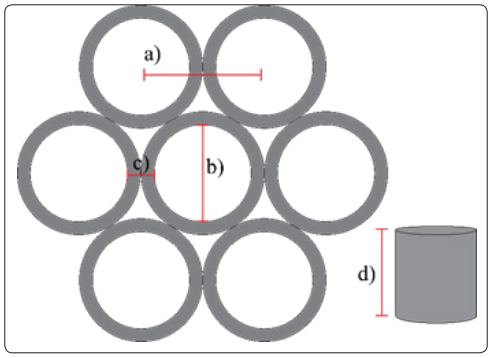

Figure 1: Geometrical parameters: a) Center to center distance between tubes, b) Inner diameter, c) Wall thickness, d) Length tube

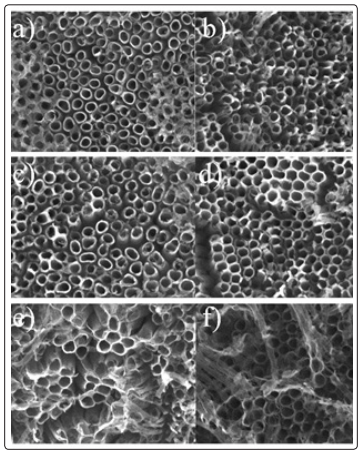

Figure 2: Top View, Scanning Electron Microscopy (SEM) micrographs of TiO_2 nanotube layers by anodization under constant voltage (30 V) in ethylene glycol, D.I. water and NH4F, a) 10 min, b) 20 min, c) 30 min, d) 40 min, e) 50 min, f) 60 min

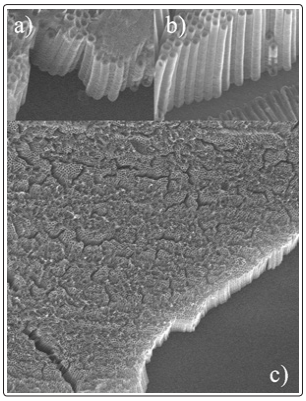

Figure 3: Perspective SEM micrograph of anodized samples by a) 10 min with tube length 284-335 nm, b) 50 min with tube length 641-679 nm, c) distant perspective to see a clean nanotube matrix. The tube length has a strong relation with anodizing time.

Through Raman spectra, it confirmed the change from an amorphous state to anatase phase, as result of annealing process. As per literature reports, there are six Raman active modes of anatase phase: A_{1g} (515cm^{-1}), $2B_{1g}$ (400 and 519 cm$_{-1}$), $3E_g$ (144, 197 and 640cm^{-1}) [22]. Figure 4 place these six Raman modes and here is important to remark the $E_{g(1)}$ theoretical position 144 cm^{-1} (indicated by vertical dashed line) for TiO_2 films and TiO_2 nanotubes [23,24].

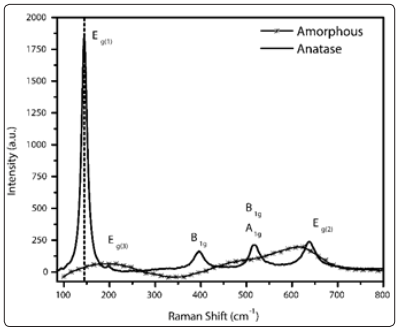

Figure 4: Raman Spectra of as-anodized amorphous sample (cross symbol line) and after annealing treatment to 400 °C (solid line) for 20 minutes

Table 1 summarizes parameters obtained by Raman spectroscopy, specifically for $E_{g(1)}$, where it is a good way to appreciate how the intensity in signal suffers an increment, due to increment in oxide thickness, it is progressive as a time function; moreover, a change takes place in $E_{g(1)}$ peak position, for 10 to 20 minutes of anodizing time, $E_{g(1)}$ appears in 142 cm^{-1}; for time = 30 min, this peak suffers a blue shift to 143 cm^{-1} position; finally, in a time lapse from 40 to 60 minutes, $E_{g(1)}$ remains in the same position as in 30 min.

Alhomoudi et al. explained this relation between Eg shift, Raman intensity and oxide thickness, so that when thickness increases, the decreasing of $E_{g(1)}$ shift takes place, until standard position (144 cm^{-1}) and this displacement is due to stress between substrate and oxide layer [25]. Similar behavior has been related to the confinement effects in nanostructured anatase crystallites [26].

Table 1: Time, $E_{g(1)}$ Shift and $E_{g(1)}$ intensity of TiO_2 nanotubes films, these parameters have been obtained from Raman spectroscopy [27].

Time (min)	*$E_{g(1)}$ position (cm^{-1})*	*$E_{g(1)}$ Raman Intensity(a.u.)*
10	142	1245
20	142	1869
30	143	2588
40	143	3268
50	143	3489
60	143	4396

Figure 5 compares the tube length and Raman intensity from examined SEM images in Figure 4 and spectra in Figure 3, both as a time function under same voltage and electrolyte conditions, from 10 to 60 minutes; here it is possible to confirm that Raman intensity has a strong relation with tube length, similar progressive behavior with this time increment.

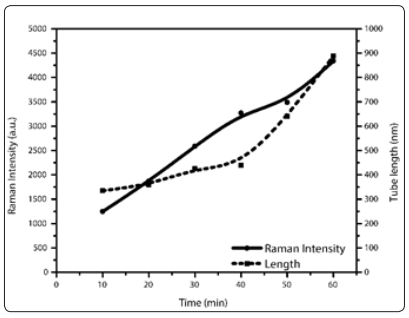

Figure 5: Comparative between Raman intensity signal (black solid circles, solid line) and tube length (black solid squares, dash line). Progressive and similar behavior for both lines

Table 2 summarizes the main parameters of the nanotubes grown, such as inner diameter or pore diameter (dp) of the tube, outer diameter (Dt), center to center distance between tubes (l), wall thickness (w) and tube length (L), these parameters was obtained using SEM images. The dp and Dt values increment with increasing time and potential.

Table 2: Main parameters of the nanotubes grown obtained from SEM images

Time (min)	*dp (nm)*	*Dt (nm)*	*L (nm)*	*w (nm)*	*L (nm)*
10	40.5	75.6	65	17.55	335
20	44.3	80.4	67	18.05	359
30	52	85.4	75	16.7	426
40	52	92	68	20	439
50	62	97	73	17.5	583
60	58	92	93	17	641

From geometric and morphological data, the surface roughness factor (R_f) and film porosity (P) of a vertical TiO_2 nanotube array can be calculated using (1) and (2) equations, where the gaps between nanotubes can be ignored according to Regonini et al. Figure 6 presents both results as time function and it is possible to observe an almost constant behavior until 60 minutes, where R_f suffers a reduction and porosity has an increment [28].

$$P = \left(1 - 2\pi \frac{dp + w^2}{\sqrt{3}\ l^2}\right) x100\% \quad (1)$$

$$R_f = \frac{4\pi}{\sqrt{3}} \frac{dp + w}{l^2} \quad (2)$$

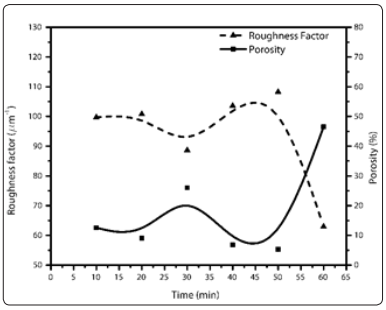

Figure 6: Calculated roughness factor (dash line) and porosity (solid line) of the whole set of anodized samples, using inner diameter, center to center distant between tubes and wall thickness

Conclusion

Amorphous TiO_2 nanotube matrix produced by titanium foils anodic oxidation, can be crystallized into pure anatase phase through an annealing process under 400 °C for high performance applications. As a main goal in this study, we observed and analyzed, from SEM images, the time lapse where it is possible to have nanotubes without presence of nanograss, and with no use of cleaning mechanical procedures, this time lapse was 10 to 40 minutes, due to the time of anodizing and constant voltage, these nanotubes are no too large, but these NTs can still be useful e.g. Surface-Enhanced Raman Spectroscopy (SERS) applications. It was observed a dependence on time of Raman intensity and $E_{g(1)}$ Shift , increasing for the first and decreasing for the second, respectively. After observation and data analysis of SEM and Raman spectroscopy, we can conclude that tube length and Raman intensity have a similar behavior, both increasing with the time pass.

Conflict of Interest

The authors confirm that this article content has no conflict of interest.

Acknowledgements

The authors are grateful to Centro de Investigación en Micro y Nanotecnología (MICRONA), Master of Science Daniel de Jesús Araujo Pérez, Engineer Rebeca Cristal Rodríguez Jiménez and Diana Balanyuk, for their help in this research.

References

1. Guisbiers, G (2010) Size-Dependent Materials Properties Toward a Universal Equation. Nanoscale Research Letters 5: 1132-1136.
2. Ge M, Cao C, Huang J, Li S, Chen Z Zhang K, et al. (2016) A review of one-dimensional TiO_2 nanostructured materials for environmental and energy applications. Journal of Materials Chemistry A 4: 6772-6801.
3. Rao B, Torabi A, Varghese O (2016) Anodically grown functional oxide nanotubes and applications. MRS Communications 6: 375-396.
4. Lamberti A, Virga A, Chiadò A, Chiodoni A, Bejtka K, et al. (2015) Ultrasensitive Ag-coated TiO_2 nanotube arrays for flexible SERS-based optofluidic devices. Journal of Materials Chemistry C 3: 6868-6875.
5. Sun Z, Liao T, Kou L (2016) Strategies for designing metal oxide nanostructures. Science China Materials 60: 1-24.
6. Yang W, Yu Y, Starr MB, Yin X, Li Z, et al. (2015) Ferroelectric polarization-enhanced photoelectrochemical water splitting in TiO_2–$BaTiO_3$ core–shell nanowire photoanodes. Nano Letters15: 7574-7580
7. Grätzel, M (2001) Photoelectrochemical cells. Nature 414: 338-344.
8. Yajun J (2014) Growth mechanism and photocatalytic performance of double-walled and bamboo-type TiO_2 nanotube arrays. RSC Advances 4: 40474-40481.
9. Popat K, Leoni L, Grimes C, Desai T (2009) Influence of engineered titania nanotubular surfaces on bone cells. Biomaterials 28: 3188-3197.
10. Fadlallah M (2017) Magnetic, electronic, optical, and photocatalytic properties of nonmetal and halogen-doped anatase TiO_2 nanotubes. Physica E: Low-dimensional Systems and Nanostructures 89: 50-56.
11. Gong D, Grimes C, Varghese O, Hu W, Singh R, et al. (2001) Titanium oxide nanotube arrays prepared by anodic oxidation. Journal of Materials Research 16: 3331-3334.
12. Jin R, Liao M, Lin T, Zhang S, Shen X, et al. (2017) Formation and evolution of anodic TiO_2 nanotube embryos. Materials Research Express 4: 6.
13. Chernozem R, Surmeneva M, Surmenev R (2016) Influence of Anodization Time and Voltage on the Parameters of TiO_2 Nanotubes. IOP Conference Series: Materials Science and Engineering 116: 012025.
14. Gui Q, Yu D, Li D, Song Y, Zhu X, et al. (2014) Efficient suppression of nanograss during porous anodic TiO_2 nanotubes growth. Applied Surface Science 314: 505-509.
15. T. Hoseinzadeh, Z. Ghorannevis, M. Ghoranneviss (2017) Effect of different electrolyte concentrations on TiO_2 anodized nanotubes physical properties. Applied Physics A: Materials Science and Processing 123: 436.
16. Ya J, Li A, Liu Z, Lei E, Zhao W, et al. (2011) Investigation of surface morphologies of TiO_2 nanotube arrays by anodization in ethylene glycol electrolytes. Journal of optoelectronics and advanced materials 13: 684-688.
17. Smith Y, Ray R, Carlson K, Sarma B, Misra M (2013) Self-Ordered Titanium Dioxide Nanotube Arrays: Anodic Synthesis and Their Photo/Electro-Catalytic Applications. Materials 6: 2892-29547.
18. Banerjee S, Pillai S, Falaras P, O'Shea K, Byrne J, et al. (2014) New Insights into the Mechanism of Visible Light Photocatalysis. The Journal of Physical Chemistry Letters 5: 2543-2554.
19. Zhu K, Neale N, Miedaner A, Frank A (2014) Enhanced charge-collection efficiencies and light scattering in dye-sensitized solar cells using oriented TiO_2 nanotubes arrays. Nano Letters 7: 69-74.
20. Yin Y, Jin Z, Hou F, Wang X (2007) Synthesis and morphology of TiO_2 nanotube arrays by anodic oxidation using modified glycerol-based electrolytes. Journal of the American Ceramic Society 90: 2384-2389.
21. Zhu K, Vinzant T, Neale N, Frank A (2007) Removing Structural Disorderfrom Oriented TiO_2 Nanotube Arrays: Reducing the Dimensionality of Transport and Recombination in Dye-Sensitized Solar Cells. Nano Letters 7: 3739-3746.
22. Ohsaka, T; Izumi, F; Fuji, Y. Raman spectrum of anatase, TiO_2. Journal of Raman Spectroscopy, 1978, 7, 321-324.
23. Zakharova G (2014) TiO_2 (Anatase) Films Nanotubes. Russian Journal of Inorganic Chemistry 59: 148-153.
24. Alhomoudi I, Newaz G (2009) Residual stresses and Raman shift relation in anatase TiO_2 thin film. Thin Solid Films 517: 4372-4378.
25. Mao Y, Wong S (2006) Size- and Shape-Dependent Transformation of Nanosized Titanate into Analogous Anatase Titania Nanostructures. Journal of the American Chemical Society 128: 8217-8226.
26. Xue X, Ji W, Mao Z, Mao H, Wang Y, et al. (2012) Raman Investigation of Nanosized TiO_2: Effect of Crystallite Size and Quantum Confinement. The Journal of Physical Chemistry C 116: 8792-8797.
27. Zhu K, Neale N, Miedaner A (2007) Enhanced charge-collection efficiencies and light scattering in dye-sensitized solar cells using oriented TiO_2 nanotubes arrays. Nano Letters 7: 69-74.